Published in final edited form as:

ACS Nano. 2019 October 22; 13(10): 11273–11282. doi:10.1021/acsnano.9b04384.

Needle-Free Injection of Exosomes Derived from Human Dermal Fibroblast Spheroids Ameliorates Skin Photoaging

Shiqi Hu[†,‡], **Zhenhua Li**[†,‡], **Jhon Cores**[†,‡], **Ke Huang**[†], **Teng Su**[†,‡], **Phuong-Uyen Dinh**[†,‡], **Ke Cheng**[*,†,‡]

[†]Department of Molecular Biomedical Sciences and Comparative Medicine Institute, North Carolina State University, Raleigh, North Carolina 27607, United States

[‡]Joint Department of Biomedical Engineering, University of North Carolina at Chapel Hill, Chapel Hill, North Carolina 27599, United States, and North Carolina State University, Raleigh, North Carolina 27606, United States

Abstract

Human dermal fibroblasts (HDFs), the main cell population of the dermis, gradually lose their ability to produce collagen and renew intercellular matrix with aging. One clinical application for the autologous trans-dermis injection of HDFs that has been approved by the Food and Drug Administration aims to refine facial contours and slow down skin aging. However, the autologous HDFs used vary in quality according to the state of patients and due to many passages they undergo during expansion. In this study, factors and exosomes derived from three-dimensional spheroids (3D HDF-XOs) and the monolayer culture of HDFs (2D HDF-XOs) were collected and compared. 3D HDF-XOs expressed a significantly higher level of tissue inhibitor of metalloproteinases-1 (TIMP-1) and differentially expressed miRNA cargos compared with 2D HDF-XOs. Next, the efficacy of 3D HDF-XOs in inducing collagen synthesis and antiaging was demonstrated *in vitro* and in a nude mouse photoaging model. A needle-free injector was used to administer exosome treatments. 3D HDF-XOs caused increased procollagen type I expression and a significant decrease in MMP-1 expression, mainly through the downregulation of tumor necrosis factor-alpha (TNF-α) and the upregulation of transforming growth factor beta (TGF-β). In addition, the 3D-HDF-XOs group showed a higher level of dermal collagen deposition than bone marrow mesenchymal stem cell-derived exosomes. These results indicate that exosomes from 3D cultured HDF spheroids have anti-skin-aging properties and the potential to prevent and treat cutaneous aging.

Graphical Abstract

[*]**Corresponding Author** kcheng3@ncsu.edu.

ASSOCIATED CONTENT

Supporting Information

The Supporting Information is available free of charge on the ACS Publications website at DOI: 10.1021/acsnano.9b04384.

Extra experimental methods, antibodies used in this study, raw Western blot data, miRNA array data, and supplementary figures (PDF)

The authors declare no competing financial interest.

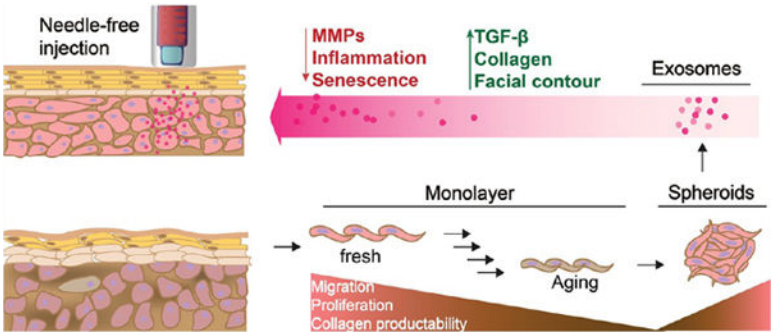

Keywords

needle-free injection; dermal fibroblasts; spheroids; exosomes; skin aging; microRNA

There is a contradiction between irreversible aging and human beings' permanent pursuit of a healthy and young appearance. Many efforts have been made to fight against skin aging as people's cosmetic desires increase. Various materials, such as antioxidants, retinoids,[1] peptides,[2] and growth factors[3] have been used to protect or repair the skin. Dermal fillers have proven more effective at smoothing facial contours and much longer lasting than topical treatments.[4] Autologous patient fat or collagen are relatively safe filler materials. Unfortunately, they are tedious to harvest and easily resorbed by the body within several months. Autologous dermal fibroblast injections are capable of improving facial contour defects and creating a continuous protein repair system (12−48 months)[5,6] to reduce wrinkle formation. However, fibroblasts gradually lose their capacity to proliferate and synthesize collagen with aging. Both intrinsic and extrinsic aging change the quantity and proliferation rates of dermal fibroblasts, reduce collagen production, and accelerate the degradation of the dermal matrix by matrix-degrading metalloproteinases (MMPs), thereby inducing wrinkles.

Exosomes have recently received much scientific attention since they can mediate cell-to-cell communication and regulate the properties of target cells. For example, exosomes derived from human induced pluripotent stem cells (iPSCs)[7] were reported to significantly reduce the expression level of MMPs and senescence-associated beta-galactosidase (SA-β-Gal) and upregulate the expression of collagen in HDFs. The epidermis layer is 50–120 μm and the epidermis−dermis thickness is 2−5 mm in humans.[8] Topical treatment with exosomes can reach the epidermis and be absorbed on human skin;[9] however, the efficiency is largely limited due to poor penetration through the stratum. A needle-free injector has been widely used for local anesthesia and vaccine delivery in humans due to its safety and efficacy,[10] especially for needle-phobic patients. A needle-free jet injector can easily deliver intact phospholipid vesicles across the skin[11,12] and could be a cosmetic device for exosome delivery.

In this study, the three-dimensional (3D) culture of human dermal fibroblast (HDF) spheroids was developed to stimulate the expression of a selected group of cytokines and to help photoaged HDFs regain their collagen synthesizing ability. To induce photoaging *in vitro* and *in vivo*, dermal fibroblasts and nude mice were irradiated with ultraviolet B light

(UVB, 311 nm). In addition, associated signal pathways were analyzed by Western blot to address the biological processes possibly linked to the specific alterations of proteins and miRNA cargos in exosomes.

RESULTS AND DISCUSSION

Comparison of Monolayer HDFs and Spheroids.

Dermal fibroblasts are the predominant mesenchymal cell type for extracellular matrix deposition and remodeling.[13] Intrinsic and extrinsic aging, however, greatly reduce the ability of HDFs to proliferate and generate collagen, which in turn accelerates the breakdown of connective tissue and generates wrinkles. In this study, HDFs were obtained commercially and expanded. HDF spheroids were formed by passaging HDFs into ultralow attachment tissue culture flasks.[14] As shown in Figure 1A, the morphology of HDFs in a monolayer is a classic spindle-like shape. The spheroids are compact aggregates of HDFs cultured in suspension. They have diameters of 100−200 μm and higher expressions of the proteins vimentin and CD34 (Figure 1B). Vimentin expression is highly related to fibroblast growth and collagen accumulation,[15] while $CD34^{pos}$ fibroblasts[16] exhibit enhanced *in vitro* invasion and migration, which means that these cells retain, and even enhance, their proliferative ability when cultured in 3D spheroids. As illustrated in Figure 1C, along with intrinsic aging (passage) and extrinsic aging (UVB) on 2D HDFs, partial cells were cultured into ultralow attachment flasks to form corresponding 3D HDFs. Besides vimentin and CD34, the secretions from cells growing in suspended spheroids differed greatly from those of monolayer cultured cells. For example, vascular endothelial growth factor (VEGF) expression in HDFs was reported to be 22-fold higher in the three-dimensional culture system.[17] In this study, type I procollagen expression was detected using an enzyme-linked immunosorbent assay (ELISA). Type I procollagen is a precursor to type I collagen, which is the major structural protein in skin connective tissue.[18] An emerging body of evidence suggests that dermal fibroblasts gradually lose their ability to produce type I procollagen by oxidative metabolism from UV irradiation and constant passaging-driven senescence.[19] Figure 1D shows that after passaging and UVB irradiation, the procollagen type I synthesis ability of 2D HDFs was greatly suppressed. However, spheroids were able to restore the type I procollagen production of HDFs. Thus, 3D culture is a potential approach to investigate a possible strategy to prevent skin aging.

Then, we analyzed the secretomes from different cells to explore possible components that might be effective against aging. In recent years, many studies have examined the effects of stemcell-derived conditioned medium in wound healing[20] and ischemic injury,[21] mainly because they can suppress inflammation and promote angiogenesis.[21,22] Conditioned medium from bone-marrow-derived mesenchymal stem cells (BMMSC) was demonstrated to markedly reduce UV-induced MMP1 expression and increase procollagen synthesis.[23] Thus, stemcell-conditioned medium may have antiaging agents that can be used to rejuvenate aged skin. In this study, to find out if 3D spheroids can regain the stemness of dermal fibroblasts and if the overexpressed factors or miRNAs are similar to stem cells, MSCs are used for comparison. We compared the growth factors secreted by fresh HDFs and MSCs. As shown in Figure S1, stem cells produce a series of growth factors, such as

VEGF, epidermal growth factor (EGF), insulin-like growth factor binding protein (IGFBP), and basic fibroblast growth factor (bFGF). These cytokines have been shown to contribute to angiogenesis and injury repair. Compared to MSCs, HDFs produce growth factors that are more related to collagen synthesis and dermal matrix remodeling, such as TIMP1 and TIMP2, which act as inhibitors of MMPs. Thus, as evidenced by the conditioned medium contents, dermal fibroblasts may be more potent to regulate skin tissue compared to MSCs.

Characterization of Exosomes from 2D HDFs, 3D HDFs, and MSCs.

Studies have demonstrated that exosomes derived from conditioned medium are rich in various miRNAs and proteins which mediate the intercellular communication and the functions of HDFs, including proliferation, collagen production, and DNA repair.[7,24] We isolated exosomes from the conditioned medium of 2D HDFs, 3D HDFs, and MSCs to examine their effect on HDFs. Exosomes were characterized in terms of size distribution, zeta potential, and surface marker expressions (Figure S2). The mean particle diameters of MSC-XOs, 2D HDF XOs, and 3D HDF XOs were 97, 162, and 151 nm, respectively. All exosomes were positive for EV markers tetraspanins (CD81) and multivesicular body synthesis proteins (Alix). Analysis of miRNA cargo and proteomics was subsequently conducted.

Cytokine arrays (Figure 2A) showed that the most significantly enhanced protein in 3D HDF-XOs was TIMP1, which aids in the maintenance of collagen fibers. In addition, TGF-β1 was overexpressed, and MMP1 and MMP9 were downregulated compared to 2D HDF-XOs. There was no significant difference for other proteins. The miRNAs of exosomes from MSCs have been explored for years. They are involved in the *Wnt* signaling pathway,[25] TGF-β signaling pathway,[26] and mitogen-activated protein kinase (MAPK) signaling pathway[27] in the wound healing process and anti-skin aging. In this pro-fibrosis-related miRNA array, MSC-XOs showed a higher expression of miRNAs from the miRNA29 family. The miRNAs in this family have been identified as potential post-transcriptional regulators of collagen genes. Moreover, these miRNAs are downstream of most of the profibrotic molecules produced, such as TGF-β.[28] In 3D HDF-XOs, hsa-miR-196a-5p, and hsa-miR-744–5p were downregulated compared to 2D HDF-XOs, while hsa-miR-133a3p, hsa-miR-223–3p, hsa-5011–5p, hsa-miR-325, hsa-miR-199b5p, and hsa-miR-34a-5p were upregulated compared to both MSC-XOs and 2D HDF-XOs (Figure 2B). We sought to test the hypothesis that 3D cell culture would regain the stemness of dermal fibroblasts by upregulating miRNAs found in MSCs. Indeed, our results indicated that 2D HDF-XOs were more culture was able to upregulate different miRNAs that are similar to exosomes from MSCs. This suggests that 3D cell important for tissue repair. Downregulated miR-196a would lead to a high expression of type I collagen[29] in dermal fibroblasts. MiR-223 mimics were reported to alter the levels of different cytokines[30] in the supernatant of cultured macrophages, such as enhancing IL-8 and IL-10 expression and decreasing TNF-α levels. Upregulated miR-133a[31] was reported to downregulate pro-inflammatory cytokines. These results demonstrate that these exosomes would affect skin tissue through different signaling pathways and deliver different messages to dermal fibroblasts and other cells, such as keratinocytes[32,33] and macrophages.[34]

Effects of Different Exosomes on the Proliferation and Migration of HDFs.

We investigated the effects of exosomes from three different types of cells on the proliferation, migration, and function of HDFs *in vitro*. The migration of HDFs was investigated with a wound healing assay (Figure 4A,B). Compared to the control group (serum-free medium), all treated groups showed a significantly faster rate of wound recovery. At day 3, 3D HDF-XOs and MSC-XOs showed a full recovery, while 2D HDF-XOs showed a relatively slower migration. The assessment of their effect on HDF proliferation was performed by a CCK8 assay. As shown in Figure 4C, similar to the wound healing assay, both 3D HDF-XOs and MSC-XOs significantly promoted the proliferation of HDFs compared to the control group and 2D HDF XOs. Then, UVB irradiation was used to further induce the senescent phenotype of HDFs. As shown in Figure S3, there were limited $Ki67^{pos}$ HDFs after the irradiation. However, after incubation with 3D HDF-XOs, the expression of Ki67 was significantly increased. We also used SA-β-gal to directly stain the senescent HDFs after UVB irradiation. As shown in Figure S4, UVB irradiation induced a severe senescent phenotype of HDFs (bluish color). 2D HDF-XOs cannot reverse the senescence process; however, the addition of 3D HDF-XOs or MSC-XOs significantly prevented the induction of the senescent phenotype. In the future, we will explore the reversal process of the senescent phenotype by 3D HDF-XOs and MSC-XOs to fully understand the mechanisms of skin antiaging and repair cell damage by UVB irradiation, since skin aging is not only about wrinkle formation; detecting senescent cells in skin is of interest for age-related skin pathologies and skin cancer.[35]

Collectively, we concluded that 3D culture could help reverse the signs of photoaging and achieve similar results to MSC-XOs *in vitro*. All these results suggest that the 3D culture of HDF spheroids is a vital step to regain the functional characteristics of passaged fibroblasts and that exosomes derived from dermal fibroblast spheroids help mediate the process.

Effectiveness of Exosome Delivery with a Needle-Free Injector.

To effectively regulate skin tissue, exosomes must penetrate through the epidermis to reach the dermis. While topical treatments are the most common approach used to relieve skin aging, the efficacy of these treatments is poor due to lack of sufficient penetration into the deep dermis.[36] Transdermal injections using syringes can lead to bumps and local tissue trauma. Needle-free injection technology has already highly benefited mass immunization programs[10] due to its ability to bypass possible needle stick injuries, its reusability, and the avoidance of needle phobia. Herein, we evaluated the efficacy of a commercially available jet injector, a needle-free injector, that pneumatically accelerates exosome solution into the dermis of skin (Figure 4A). Figure 4B summarized the advantages of needle-free injectors over traditional syringes, including less injury and pain, better penetration and absorption, and better suitability for cosmetic usage. 3D HDF-XOs were labeled with DiD (1,1′-dioctadecyl3,3,3′,3′-tetramethylindodicarbocyanine, 4-chlorobenzenesulfonate salt) to facilitate the detection of their distribution in the dermis. We examined the dispersion of exosomes through the histological analysis of skin biopsies (Figure 4C–E). The injection of a concentrated mass of exosomes with the syringe led to accumulation. Compared to syringe injections, the jet injector caused only invisible microtrauma to the dermis, which was beneficial since microtrauma triggers natural wound healing processes and augments

collagen generation therein.[37] As shown in Figure 4E, a mass of inflammatory cells will migrate and group to areas treated with needle injections, but jet injections induce no visible injuries.

Effects of Exosome Application in Nude Mice with UVB-Induced Skin Photoaging.

Next, we evaluated the efficacy of exosome treatment on reversing wrinkles in a nude mouse model. Repeated exposure to UV radiation injures the stratum corneum, accelerates aging, increases the risk of skin cancer,[38] and produces reactive oxygen species, which upregulate MMPs and proinflammatory cytokines that damage the dermis, thereby leading to photoaging.[39] After 8 weeks of UVB exposure (every other day), mice were randomized into five treatment groups: control, 0.05% retinoic acid (RA, positive control), 2D HDF-XOs, 3D HDF-XOs, and MSC-XOs. After the treatment, we recorded the body weight of mice every other day. Notably better skin contours were observed in the 3D HDF-XOs-treated group starting from week 3; thus, we assessed the state of the skin using skin replicas, H&E, and Masson Trichrome staining on week 4.

The effects of exosomes on wrinkle formations after UVB irradiation were investigated on the dorsal skin of mice. As shown in Figure 5, there were almost no wrinkles in the sham group. Skin replicas were imaged and analyzed to compare the number and thickness of wrinkles. In contrast, deep and wide wrinkles form in the control group due to UVB irradiation. With the treatment of exosomes by jet injection or 0.05% RA, the wrinkles in the treated groups were more superficial and thinner. RA is the bioactive metabolite of vitamin A. It has been proven effective in the treatment of photoaged skin and is approved for clinical use.[40] Usually, it will take two months to see the effect of RA treatment on mice since it is topical; the absorption and efficiency are quite limited. For exosomes, we directly delivered them into the dermis by the jet injector, which is much more efficient than topical treatment. The single treatment started to show visible effects 3 weeks after treatment. Overall, the efficacy of 2D HDF-XOs was not comparable to RA, showing many superficial fine wrinkles. MSC-XOs showed a much better antiwrinkle efficacy than RA, while 3D HDF-XOs provided the best skin treatment, leading to significantly thinner and more superficial wrinkles.

Skin histology elucidated the effects that exosomes had on the structural changes and the amount of collagen deposition in the dorsal skin (Figure 6). Masson's Trichrome staining showed the changes in the quantity of collagen in the dermis. The sham group displayed regularly arranged collagen fibers. Compared with the sham group, UV irradiation caused large amounts of abnormal, fragmented, and disorganized collagenfibers in the UV control group. Additionally, more inflammatory cells can be seen in the skin tissue of the UV control group than in other groups. Significant histological changes such as a woven stratum corneum and the disruption of collagen were observed in the control group. All treated groups showed improvements in UV-induced damage to collagen fibers. Of all the treatments, 3D HDF-XOs resulted in the most abundant and dense collagen fibers, the most compact stratum corneum, and the thinnest epidermal layers compared to the control group. We used the nude mouse as the animal subject because it does not have an immune response

to the exosome treatment. Future studies using immunocompetent animals need to be carried out to determine possible immunogenicity against injected exosomes.[41]

Effects of Exosome Treatment on MMP-1 and Type I Procollagen Expression.

To determine the molecular mechanisms of 3D HDF-XOs driven amelioration of skin aging and collagen degradation in a UV-induced skin-aging nude mouse model, we performed an apoptosis protein array on skin samples after treatment. As shown in Figure S5, the 3D HDF-XOs treatment group showed fewer apoptotic and inflammatory factors, such as Fas ligand, IFN-γ, and IL-1β, and higher expressions of TIMP-1 and TIMP-2. From these data, we can see that the treatment efficacy of 3D HDF-XOs partially comes from reduced inflammation and the suppression of MMPs. Thus, we further investigated type I procollagen, MMP-1, IL-1β, and TGF-β expression of all groups using Western blotting (Figure 7A–F). Both UV-induced photoaging and intrinsic aging reduced type I procollagen synthesis by blocking the TGF-β signaling pathway and enhanced inflammation and MMP synthesis by upregulating TNF-α.[42,43] The synthesis of procollagen was significantly enhanced, and the TGF-β signaling pathway was activated for all treatment groups, especially for the MSC-XOs and 3D HDF-XOs groups. The expression of type I procollagen and TGF-β in the 3D HDF-XOs group was significantly higher than in the MSC-XOs group. Meanwhile, the expression of MMP-1 was decreased to normal levels in groups after treatment with MSC-XOs and 3D HDF XOs compared with the control group. RA and 2D HDF-XOs showed a limited repair and regulation capacity. The expressions of IL-1β and TNF-α were drastically increased in the UVB-irradiated control group, which means a higher level of inflammation, MMPs, and senescence. For MSC-XOs and 3D HDF-XOs, they both ameliorated the inflammation induced by UV irradiation and activated TGF-β. MSC-XOs are well known for their ability to reduce inflammation, accelerate skin cell migration, improve angiogenesis, and even ameliorate skin aging.[44] In this study, 3D HDF-XOs induced dermal fibroblasts to produce more procollagen and TIMP-1 to inhibit collagen degradation. Figure 7G shows the possible mechanisms of 3D HDF-XOs in anti-skin aging. UV light induced the enhanced oxidative stress in the skin, which activated the TNF-α and NF-κB signaling pathways, leading to the degradation of collagens and senescence consequently. Overall, this study indicated that the 3D HDF-XOs group is the most effective in protecting skin from photoaging. In particular, TIMP-1 and TGF-β, which are important in MMP suppression and regulating matrix synthesis, were upregulated, while TNF-α was downregulated.

CONCLUSIONS

Both extrinsic and intrinsic aging lead to a microenvironment with enhanced oxidative stress and inflammatory levels, as well as senescent dermal fibroblasts. During the aging process, the upregulation of MMP production and the downregulation of collagen production lead to age-related skin disorders, including weakened dermal structure and poor mechanical integrity. Our findings indicate that spheroid formation can restore the function of aged HDFs. In addition, our findings indicate that 3D HDF-XOs may regulate dermal fibroblasts to induce efficient collagen biosynthesis and ameliorate inflammation in the skin caused by UVB irradiation. Thicker dermal matrix was successfully achieved in nude mice using

needle-free injections of 3D HDF-XOs. The results of the miRNA profiling data herein indicate that the downregulation of miR196a, as well as the upregulation of miR-133a and miR-223, might contribute to the process. 3D HDF-XOs inhibited UVB-induced MMP1 expression, restored type I procollagen, and activated the TGF-β signal pathway. In addition, 3D HDF-XOs ameliorated the inflammation and senescence of the skin through the downregulation of TNF-α.

In conclusion, needle-free injections of exosomes with a jet injector provide an effective approach for transdermal delivery of exosomes. 3D HDF-XOs were more effective than MSC-XOs at regulating dermal fibroblast proliferation, migration, and protein expression, thus reducing skin aging.

EXPERIMENTAL SECTION

Cells and Exosomes.

Normal human dermal fibroblasts (PCS201012) (ATCC, Manassas, VA, USA) were cultured in Dulbecco's modified Eagle's medium (DMEM) supplemented with a low serum growth supplement kit (S00310) (Thermo-Fisher Scientific, Rockford, IL, USA) in a cell incubator. Bone marrow-derived mesenchymal stem cells (normal, human, ATCC PCS-500012) were placed in mesenchymal stem cell basal medium (ATCCPCS-500–030) with a growth kit (ATCC-PCS-500–041). Spheroids were formed by transferring HDFs (one million cells) into ultralow attachment flasks (Corning 3815, 75 cm^2). Then, conditioned medium was collected for exosome isolation. Briefly, for monolayer cells, cells were seeded into T-175 flasks. Once the cells were 80% confluent, they were washed with phosphate-buffered saline (PBS) three times. Then, 20 mL of serum-free DMEM (for HDFs) or mesenchymal stem cell basal medium (for MSCs) were added to each T-175 flask for an additional 5 days. For HDF spheroids, the medium was replaced with serum-free DMEM on day 3 after spheroid formation. Then, the conditioned medium was collected after 5 days. For both monolayer cells and spheroids, after the incubation with serum-free DMEM, conditioned medium was collected and filtered through a 0.22 μm filter unit (SCGP00525) (Sigma-Aldrich, St. Louis, MO, USA) to get rid of cells and debris. To remove the proteins and concentrate the exosomes in the medium, the medium was then centrifuged and washed with PBS through an ultra-15 centrifugal filter unit (100 kDa, UFC910024) (MilliporeSigma, Burlington, MA, USA). The exosomes were concentrated to 10^{10}/mL and stored at −80 °C for further use.

Characterization.

The concentration of exosomes was examined by a NanoSight LM10 (Malvern Instruments Ltd., UK). The size of exosomes was measured by dynamic light scattering (DLS, Malvern ZEN 3600 Zetasizer). The morphology of exosomes was recorded using a transmission electron microscope (TEM, JEOL JEM2000FX). Total RNA of exosomes was extracted using the RNeasy Mini kit (Qiagen, Germany), and the miRNA analysis was performed with an miScript miRNA PCR array human fibrosis kit (Qiagen, Germany).

Cytokine Array.

The comparison of HDF-CM and MSC-CM was performed using a human cytokines array (AAH-CYT-1000) (RayBiotech, Peachtree Corners, GA, USA) according to the manufacturer's instructions. The cytokines of 2D HDFs and 3D HDFs were analyzed using a human angiogenesis array C1000 (RayBiotech, AAH-ANG-1000). Skin samples were analyzed using a mouse apoptosis signaling pathway array (RayBiotech, AAMAPOSIG-1).

Ultraviolet B Irradiation of HDFs.

For *in vitro* studies, HDFs were washed with PBS before the exposure to UVB. The UVB dose (Philip, 311 nm, 20W/01, Germany) was 0.05 J/cm^2/day for 3 days.

Then, cells were incubated with serum-free DMEM with or without exosomes at 10^8/mL for another 24 h.

Type I Procollagen ELISA.

Type I procollagen concentration was measured by ELISA (Abcam, Cambridge, UK). The absorbance at 450 nm was measured using a microplate spectrophotometer (BioTek Instruments, Winooski, VT, USA).

Wound Healing Assay.

The HDFs were seeded in two-well ibidi inserts (Minitube Canada, Ingersoll, Ontario) at 1 × 10^5 cells per well and cultured overnight to form a confluent monolayer at 37 °C in 5% CO_2. The inserts were then carefully removed by peeling them back from one corner, and the cells were washed with serum-free DMEM once and then maintained in serum-free DMEM with or without exosomes (10^8/mL). At 0, 24, and 48 h, the scratched areas were imaged and measured using NIH ImageJ ($n = 3$).

Proliferation Assay.

An HDF proliferation study was performed using a Cell Counting Kit-8 (96992–500TESTS-F, Sigma-Aldrich). Briefly, the HDFs were seeded at 5,000 cells per well in a 96-well plate and allowed to settle overnight. Then, the medium was replaced with serum-free DMEM with or without exosomes. After another 48 h, CCK-8 reagent was added to each well and incubated for 1 h. Absorbance at 450 nm was read and recorded using a microplate spectrophotometer.

Animal Studies.

All animal work was compliant with the Institutional Animal Care and Use Committee (IACUC) of North Carolina State University. For the topical experiment, the nude mouse dorsal skin (6−8 weeks old, The Jackson Laboratories) was irradiated with UVB every other day for 8 weeks. The irradiation intensity, represented as the minimal erythemal dose (MED), was set at 1 MED during the first 2 weeks (60 mJ/cm^2) and was elevated to 2 MED (120 mJ/cm^2) in the third week, to 3 MED (180 mJ/cm^2) in the fourth week, and to 4 MED (240 mJ/cm^2) during the fifth to eighth weeks of the experiment. The total irradiated UVB volume was approximately 80 MED. Treatment: 18 nude mice were randomly divided into

six groups of three mice each: (a) no UVB exposure (sham); (b) UVB irradiation alone (control); (c) UVB irradiation with 0.05% retinoic acid; (d) UVB irradiation with 2D HDF-XOs; (e) UVB irradiation with 3D HDF-XOs; and (f) UVB irradiation with MSC-XOs. In this experiment, 0.05% RA was used as a positive control and applied on the dorsal skin every other day. Exosomes were all delivered by Dermo-jet model G (DJ-05, Robbins Instruments, USA). Dermo-jet exosome delivery consisted of one-time injections in 10 different sites evenly on the whole dorsal skin. The exosome dose used was 10^{10}/mL and 1 mL per mouse. For each mouse, the whole back skin was divided into at least three parts to be analyzed. There were three mice for each group and there was good consistency and no significant differences within groups.

Skin Replica.

Replica SILFLO and Ring Locator were brought from Clinical & Derm, Dallas, TX, USA. Skin replica was performed at the end of the treatment on the back skin of mice. Then, the replica was observed under a stereomicroscope (Olympus SZX7), and corresponding images were analyzed by ImageJ (NIH).

Statistical Analysis.

The experimental data in this study were presented as mean ± standard deviation. Comparisons among more than two groups were performed using one-way ANOVA followed by *post hoc* Bonferroni test. Single, double, triple, and quadruple asterisks represent $p < 0.05$, 0.01, 0.001, and 0.0001, respectively. All analyses were performed using GraphPad Prism 7 software (San Diego, CA, USA).

Supplementary Material

Refer to Web version on PubMed Central for supplementary material.

ACKNOWLEDGMENTS

This work was supported by grants from the National Institutes of Health (R01 HL123920, HL137093, HL144002, and HL146153 to K.C.) and the American Heart Association (18TPA34230092 and 19EIA34660286 to K.C.).

REFERENCES

(1). Castleberry SA; Quadir MA; Sharkh MA; Shopsowitz KE; Hammond PT Polymer Conjugated Retinoids for Controlled Transdermal Delivery. J. Controlled Release 2017, 262, 1–9.

(2). Schagen S Topical Peptide Treatments with Effective Anti-Aging Results. Cosmetics 2017, 4, 16–29.

(3). Aldag C; Teixeira DN; Leventhal PS Skin Rejuvenation Using Cosmetic Products Containing Growth Factors, Cytokines, and Matrikines: a Review of the Literature. Clin., Cosmet. Invest. Dermatol. 2016, 9, 411–419.

(4). Kim JH; Kwon T-R; Hong SW; Seok J; Kim JM; Hong JY; Lee SE; Han SW; Kim BJ Comparative Evaluation of the Biodegradability and Wrinkle Reduction Efficacy of Human-Derived Collagen Filler and Hyaluronic Acid Filler. Aesthetic Plast. Surg. 2019, 43, 1095–1101. [PubMed: 30989276]

(5). Jeong JH; Fan Y; You GY; Choi TH; Kim S Improvement of Photoaged Skin Wrinkles with Cultured Human Fibroblasts and Adipose-Derived Stem Cells: a Comparative Study. J. Plast. Reconstr. Aesthet. Surg. 2015, 68, 372–381. [PubMed: 25484240]

(6). Zorin V; Zorina A; Cherkasov V; Deev R; Kopnin P; Isaev A Clinical-Instrumental and Morphological Evaluation of the Effect of Autologous Dermal Fibroblasts Administration. J. Tissue Eng. Regener. Med. 2017, 11, 778–786.

(7). Oh M; Lee J; Kim YJ; Rhee WJ; Park JH Exosomes Derived from Human Induced Pluripotent Stem Cells Ameliorate the Aging of Skin Fibroblasts. Int. J. Mol. Sci. 2018, 19, No. E1715.

(8). Oltulu P; Ince B; Kokbudak N; Findik S; Kilinc F Measurement of Epidermis, Dermis, and Total Skin Thicknesses From Six Different Body Regions with a New Ethical Histometric Technique. Turk. J. Plast. Surg. 2018, 26, 56–61.

(9). Kim YJ; Yoo SM; Park HH; Lim HJ; Kim YL; Lee S; Seo KW; Kang KS Exosomes Derived From Human Umbilical Cord Blood Mesenchymal Stem Cells Stimulates Rejuvenation of Human Skin. Biochem. Biophys. Res. Commun. 2017, 493, 1102–1108. [PubMed: 28919421]

(10). Ravi AD; Sadhna D; Nagpaal D; Chawla L Needle Free Injection Technology: a Complete Insight. Int. J. Pharm. Investig. 2015, 5, 192–199.

(11). Schlich M; Lai F; Murgia S; Valenti D; Fadda AM; Sinico C Needle-Free Jet Injection of Intact Phospholipid Vesicles Across The Skin: a Feasibility Study. Biomed. Microdevices 2016, 18, 67–73. [PubMed: 27422107]

(12). Kwon TR; Seok J; Jang JH; Kwon MK; Oh CT; Choi EJ; Hong HK; Choi YS; Bae J; Kim BJ Needle-Free Jet Injection of Hyaluronic Acid Improves Skin Remodeling in a Mouse Model. Eur. J. Pharm. Biopharm. 2016, 105, 69–74. [PubMed: 27257030]

(13). Tracy LE; Minasian RA; Caterson EJ Extracellular Matrix and Dermal Fibroblast Function in the Healing Wound. Adv. Wound Care. 2016, 5, 119–136.

(14). Ray S; Langan RC; Mullinax JE; Koizumi T; Xin HW; Wiegand GW; Anderson AJ; Stojadinovic A; Thorgeirsson S; Rudloff U; Avital I Establishment of Human Ultra-Low Passage Colorectal Cancer Cell Lines Using Spheroids from Fresh Surgical Specimens Suitable for in Vitro and in Vivo Studies. J. Cancer 2012, 3, 196–206. [PubMed: 22606209]

(15). Cheng F; Shen Y; Mohanasundaram P; Lindstrom M; Ivaska J; Ny T; Eriksson JE Vimentin Coordinates Fibroblast Proliferation and Keratinocyte Differentiation in Wound Healing via TGF-Beta-Slug Signaling. Proc. Natl. Acad. Sci. U. S. A. 2016, 113, E4320–4327. [PubMed: 27466403]

(16). Salzer MC; Lafzi A; Berenguer-Llergo A; Youssif C; Castellanos A; Solanas G; Peixoto FO; Stephan-Otto Attolini C; Prats N; Aguilera M; Martín-Caballero J; Heyn H; Benitah SA Identity Noise and Adipogenic Traits Characterize Dermal Fibroblast Aging. Cell 2018, 175, 1575–1590. [PubMed: 30415840]

(17). Pinney E; Liu K; Sheeman B; Mansbridge J Human Three-Dimensional Fibroblast Cultures Express Angiogenic Activity. J. Cell. Physiol. 2000, 183, 74–82. [PubMed: 10699968]

(18). Purohit T; He T; Qin Z; Li T; Fisher GJ; Yan Y; Voorhees JJ; Quan T Smad3-Dependent Regulation of Type I Collagen in Human Dermal Fibroblasts: Impact on Human Skin Connective Tissue Aging. J. Dermatol. Sci. 2016, 83, 80–83. [PubMed: 27132061]

(19). Cole MA; Quan T; Voorhees JJ; Fisher GJ Extracellular Matrix Regulation of Fibroblast Function: Redefining Our Perspective on Skin Aging. J. Cell Commun. Signal. 2018, 12, 35–43. [PubMed: 29455303]

(20). Pouriran R; Piryaei A; Mostafavinia A; Zandpazandi S; Hendudari F; Amini A; Bayat M The Effect of Combined Pulsed Wave Low-Level Laser Therapy and Human Bone Marrow Mesenchymal Stem Cell-Conditioned Medium on Open Skin Wound Healing in Diabetic Rats. Photomed. Laser Surg. 2016, 34, 345–354.

(21). Tang J; Shen D; Caranasos TG; Wang Z; Vandergriff AC; Allen TA; Hensley MT; Dinh PU; Cores J; Li TS; Zhang J; Kan Q; Cheng K Therapeutic Microparticles Functionalized with Biomimetic Cardiac Stem Cell Membranes and Secretome. Nat. Commun. 2017, 8, 13724. [PubMed: 28045024]

(22). Overath JM; Gauer S; Obermuller N; Schubert R; Schafer R; Geiger H; Baer PC Short-Term Preconditioning Enhances the Therapeutic Potential of Adipose-Derived Stromal/ Stem Cell-Conditioned Medium in Cisplatin-Induced Acute Kidney Injury. Exp. Cell Res. 2016, 342, 175–183. [PubMed: 26992633]

(23). Kwon TR; Oh CT; Choi EJ; Kim SR; Jang YJ; Ko EJ; Yoo KH; Kim BJ Conditioned Medium from Human Bone Marrow-Derived Mesenchymal Stem Cells Promotes Skin Moisturization and Effacement of Wrinkles in UVB-Irradiated Skh-1 Hairless. Mice. Photodermatol, Photoimmunol. Photomed. 2016, 32, 120–128. [PubMed: 26577060]

(24). Wu D; Chen JS; Chang DC; Lin SL Mir-434–5p Mediates Skin Whitening and Lightening. Clin., Cosmet. Invest. Dermatol. 2008, 1, 19–35.

(25). Rong X; Liu J; Yao X; Jiang T; Wang Y; Xie F Human Bone Marrow Mesenchymal Stem Cells-Derived Exosomes Alleviate Liver Fibrosis Through the Wnt/Beta-Catenin Pathway. Stem Cell Res. Ther. 2019, 10, 98–108. [PubMed: 30885249]

(26). Ebrahim N; Ahmed IA; Hussien NI; Dessouky AA; Farid AS; Elshazly AM; Mostafa O; Gazzar WBE; Sorour SM; Seleem Y; Hussein AM; Sabry D Mesenchymal Stem Cell-Derived Exosomes Ameliorated Diabetic Nephropathy by Autophagy Induction through the mTOR Signaling Pathway. Cells 2018, 7, No. E226.

(27). Zhao P; Xiao L; Peng J; Qian YQ; Huang CC Exosomes Derived From Bone Marrow Mesenchymal Stem Cells Improve Osteoporosis Through Promoting Osteoblast Proliferation via MAPK Pathway. Eur. Rev. Med. Pharmacol. Sci. 2018, 22, 3962–3970. [PubMed: 29949171]

(28). Banerjee J; Sen CK MicroRNAs in Skin and Wound Healing. Methods Mol. Biol. 2013, 936, 343–356. [PubMed: 23007520]

(29). Honda N; Jinnin M; Kajihara I; Makino T; Makino K; Masuguchi S; Fukushima S; Okamoto Y; Hasegawa M; Fujimoto M; Ihn H TGF-Beta-Mediated Downregulation of MicroRNA-196a Contributes to the Constitutive Upregulated Type I Collagen Expression in Scleroderma Dermal Fibroblasts. J. Immunol. 2012, 188, 3323–3331. [PubMed: 22379029]

(30). Zhou H; Xiao J; Wu N; Liu C; Xu J; Liu F; Wu L MicroRNA-223 Regulates the Differentiation and Function of Intestinal Dendritic Cells and Macrophages by Targeting C/EBPbeta. Cell Rep. 2015, 13, 1149–1160. [PubMed: 26526992]

(31). Tahamtan A; Teymoori-Rad M; Nakstad B; Salimi V Anti-Inflammatory MicroRNAs and Their Potential for Inflammatory Diseases Treatment. Front. Immunol. 2018, 9, 1377.

(32). Espada J; Matabuena M; Salazar N; Lucena S; Kourani O; Carrasco E; Calvo M; Rodríguez C; Reyes E; González S; Juarranz A Cryptomphalus Aspersa Mollusc Eggs Extract Promotes Migration and Prevents Cutaneous Ageing in Keratinocytes and Dermal Fibroblasts in Vitro. Int. J. Cosmet. Sci. 2015, 37, 41–55.

(33). Huang P; Bi J; Owen GR; Chen W; Rokka A; Koivisto L; Heino J; Hakkinen L; Larjava H Keratinocyte Microvesicles Regulate the Expression of Multiple Genes in Dermal Fibroblasts. J. Invest. Dermatol. 2015, 135, 3051–3059. [PubMed: 26288358]

(34). Zhao J; Hu L; Gong N; Tang Q; Du L; Chen L The Effects of Macrophage-Stimulating Protein on the Migration, Proliferation, and Collagen Synthesis of Skin Fibroblasts in Vitro and in Vivo. Tissue Eng., Part A 2015, 21, 982–991. [PubMed: 25315688]

(35). Wang AS; Dreesen O Biomarkers of Cellular Senescence and Skin Aging. Front. Genet. 2018, 9, 247. [PubMed: 30190724]

(36). Ng KW Penetration Enhancement of Topical Formulations. Pharmaceutics 2018, 10, No. E51.

(37). Ritti L. Cellular Mechanisms of Skin Repair in Humans and Other Mammals. J. Cell Commun. Signal. 2016, 10, 103–120. [PubMed: 27170326]

(38). Panich U; Sittithumcharee G; Rathviboon N; Jirawatnotai S Ultraviolet Radiation-Induced Skin Aging: The Role of DNA Damage and Oxidative Stress in Epidermal Stem Cell Damage Mediated Skin Aging. Stem Cells Int. 2016, 2016, 7370642.

(39). Battie C; Jitsukawa S; Bernerd F; Del Bino S; Marionnet C; Verschoore M New Insights in Photoaging, UVA Induced Damage and Skin Types. Exp. Dermatol. 2014, 23, 7–12.

(40). Darlenski R; Surber C; Fluhr JW Topical Retinoids in the Management of Photodamaged Skin: from Theory to Evidence-Based Practical Approach. Br. J. Dermatol. 2010, 163, 1157–1165. [PubMed: 20633013]

(41). Hong SB; Yang H; Manaenko A; Lu J; Mei Q; Hu Q Potential of Exosomes for the Treatment of Stroke. Cell Transplant. 2019, 28, 662–670. [PubMed: 30520322]

(42). Hwang E; Lee DG; Park SH; Oh MS; Kim SY Coriander Leaf Extract Exerts Antioxidant Activity And Protects Against UVB-Induced Photoaging Of Skin By Regulation of Procollagen Type I And MMP-1 Expression. J. Med. Food 2014, 17, 985–995. [PubMed: 25019675]

(43). Quan T; Wang F; Shao Y; Rittie L; Xia W; Orringer JS; Voorhees JJ; Fisher GJ Enhancing Structural Support Of The Dermal Microenvironment Activates Fibroblasts, Endothelial Cells, and Keratinocytes in Aged Human Skin in Vivo. J. Invest. Dermatol. 2013, 133, 658–667. [PubMed: 23096713]

(44). Ferreira ADF; Gomes DA Stem Cell Extracellular Vesicles in Skin Repair. Bioengineering 2019, 6, No. E4.

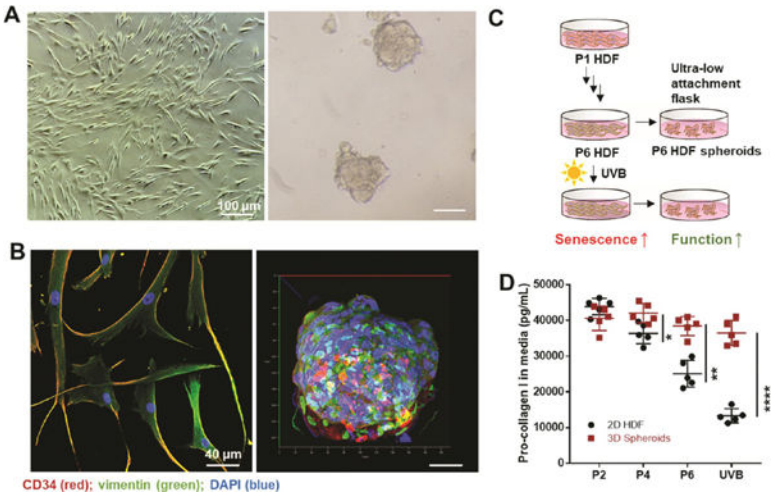

Figure 1.

Comparison of 2D HDFs and 3D spheroids. (A) Photographs of human dermal fibroblasts (HDFs) and formed spheroids (scale bar: 100 μm). (B) Evaluation of vimentin (green channel) and CD34 (red channel) expression in 2D and 3D cultured HDFs (P6). DAPI (blue) was used to locate the nuclei of the cells (scale bar: 40 μm). (C) Schematic illustration of the culture process. (D) Pro-collagen I expression in 2D HDFs and spheroids from passages 2, 4, and 6, and after UVB exposure. Expression assessed by ELISA. $n = 5$, *$p < 0.05$,**$p < 0.01$, ****$p < 0.0001$.

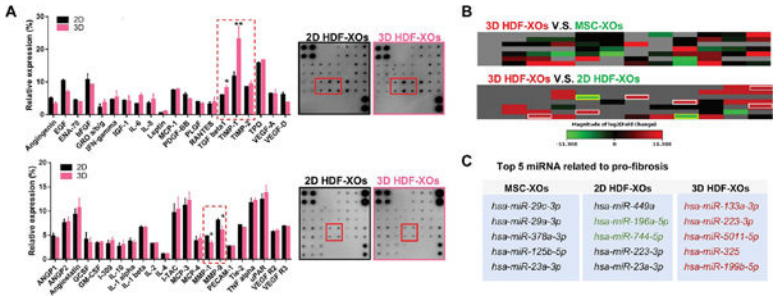

Figure 2.

Comparison of exosomes derived from MSCs and 2D and 3D HDFs. (A) Cytokine array of 2D HDF-XOs and 3D HDF-XOs (P6) by densitometric analysis ($n = 3$). (B) Heatmap of a fibrosis-related miRNA array incubated with 2D HDF-XOs, 3D spheroids-XOs, and MSC-XOs ($n = 3$). In 3D HDF-XOs, hsa-miR-196a-5p and hsa-miR-744-5p were downregulated compared to 2D HDF-XOs, while hsa-miR133a-3p, hsa-miR-223-3p, hsa-5011-5p, hsa-miR-325, hsa-miR-199b-5p, and hsa-miR-34a-5p were upregulated compared to both MSC-XOs and 2D HDF-XOs. (C) miRNAs of 2D HDF-XOs, 3D HDF-XOs, and MSC-XOs expressed at relatively high levels. $n = 3$, $^{*}p < 0.05$, $^{**}p < 0.01$.

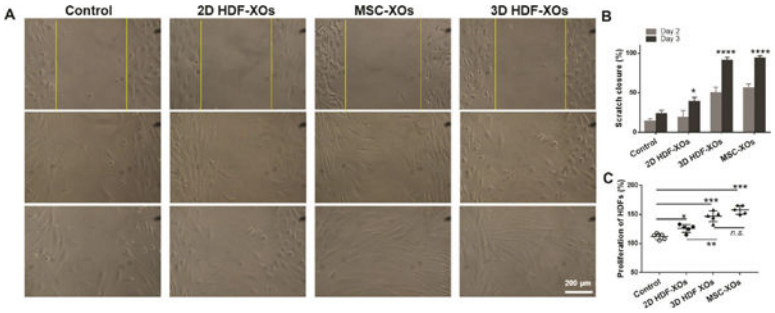

Figure 3.

Effects of exosomes on HDFs. (A) Wound recovery rates of HDFs, modeled by cell scratch assays. (B) The scratch closure rate is presented over time ($n = 3$). (C) HDF proliferation with the treatment of different exosomes, $n = 3$, n.s. means no significant difference, $*p < 0.05$, $**p < 0.01$, $***p < 0.001$, $****p < 0.0001$.

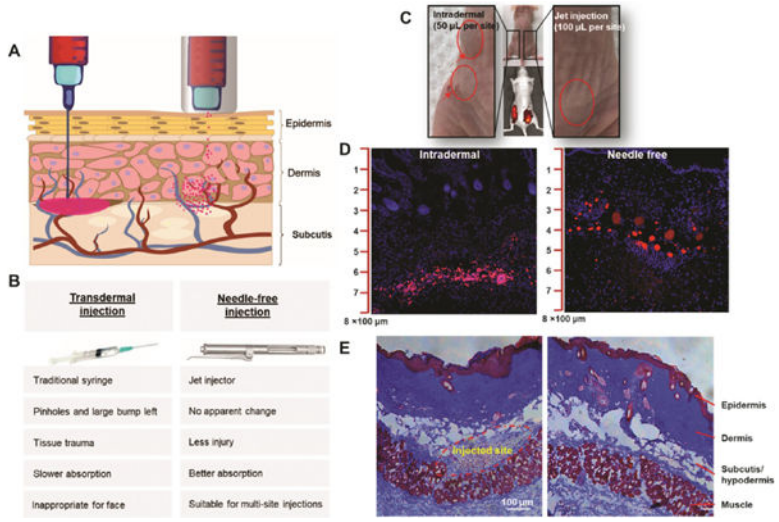

Figure 4.

Comparison of intradermal injection with a syringe to needle-free injection with a jet injector. (A) Schematic illustration of needle injection and needle-free injection. (B) Comparison of syringe and jet injector properties and applications. (C) Exosomes were labeled with DiD (1,1′-dioctadecyl-3,3,3′,3′-tetramethylindodicarbocyanine, 4-chlorobenzenesulfonate salt) and injected into the dorsal skin of a nude mouse. The intradermal injections were administered on the left side of the back. The arrows indicate the injection sites. The jet injections were administered on the right side of the back. There was no obvious administration injury. A relatively large amount of solution pools in the tissue as a result of needle injections, which leads to local tissue trauma. Jet injections result in wider penetration and better absorption. (D) The mice were sacrificed 12 h after injection. Skin slices from the left and right sites were imaged *via* confocal microscopy. Highly concentrated exosomes (red) accumulated between the dermis and hypodermis in the mice that were intradermally injected. In mice treated with the jet injector, the exosomes dispersed well in both the dermis and hypodermis. (E) Representative skin histology. Scale bar: 100 μm.

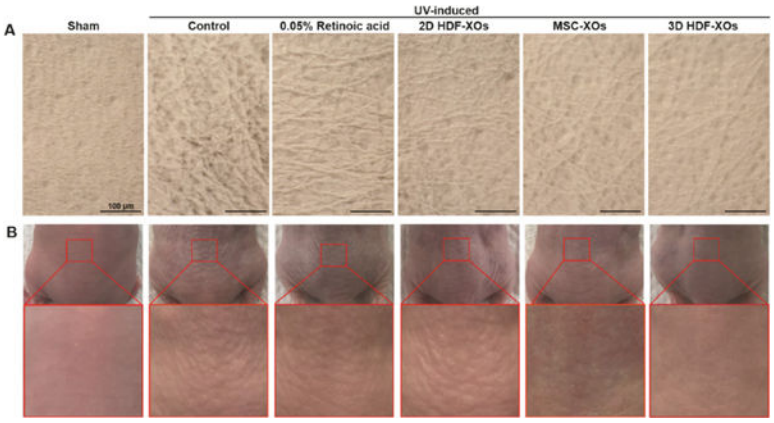

Figure 5.

Effects of retinoic acid (RA) and exosomes from different cells on wrinkle formation in UVB-irradiated nude mice. (A) Microscopic observation of replicas (scale bar: 100 μm) and (B) photographs of dorsal skin of mice from different groups (n = 3).

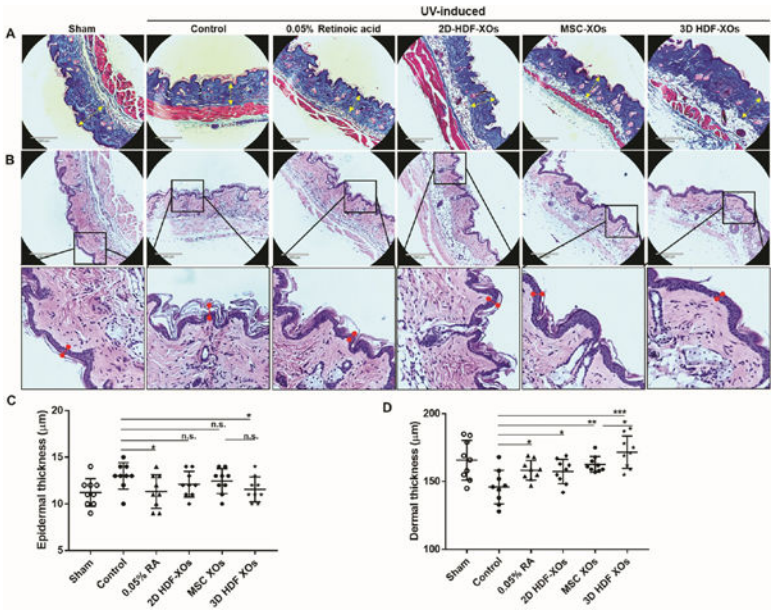

Figure 6.

Histological analysis of the dorsal surface of treated and untreated nude mice after UVB irradiation. (A) Masson's Trichrome staining. From left to right: sham, saline, dermal application of 0.05% retinoic acid (every other day), PRP, MSC-XOs/PRP, and 3D spheroids XOs/PRP (last three received one-time injections); scale bar: 290 μm. (B) Corresponding H&E staining, scale bar: 290 μm. (C) Epidermal and (D) dermal thickness analysis. $n = 9$ (3 mice per group, 3 spots analyzed for each sample), n.s. means no significant difference, $^{*}p < 0.05$, $^{**}p < 0.01$, $^{***}p < 0.001$.

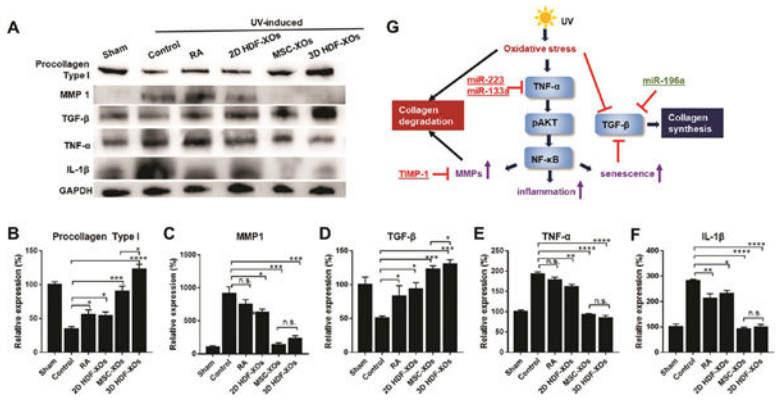

Figure 7.

Antiphotoaging mechanism signaling pathway analysis. (A) Western blot of dorsal skin of different groups. (B–F) Quantification of procollagen 1, MMP1, TGF-β, TNF-α, and IL-1β ($n = 3$); n.s. means no significant difference, *$p < 0.05$, **$p < 0.01$, ***$p < 0.001$, ****$p < 0.0001$. (G) Schematic illustration of the mechanism of 3D HDF-XOs treatment.